Pressure-Induced Hydrogen-Dominant Metallic State in Aluminum Hydride

Igor Goncharenko,[1] M. I. Eremets,[2] M. Hanfland,[3] J. S. Tse,[4,*] M. Amboage,[3] Y. Yao,[4] and I. A. Trojan[2]

[1]*Laboratoire Léon Brillouin C.E.A.-C.N.R.S., CEA Saclay, 91191 Gif-sur-Yvette, France*
[2]*Max Planck Institute für Chemie, Postfach 3060, 55020 Mainz, Germany*
[3]*European Synchrotron Radiation Facility, 38043 Grenoble, France*
[4]*Department of Physics and Engineering Physics, University of Saskatchewan, Saskatoon, Saskatchewan S7N 5E2, Canada*

(Received 23 October 2007; published 29 January 2008)

Two structural transitions in covalent aluminum hydride AlH_3 were characterized at high pressure. A metallic phase stable above 100 GPa is found to have a remarkably simple cubic structure with shortest first-neighbor H-H distances ever measured except in H_2 molecule. Although the high-pressure phase is predicted to be superconductive, this was not observed experimentally down to 4 K over the pressure range 120–164 GPa. The results indicate that the superconducting behavior may be more complex than anticipated.

DOI: 10.1103/PhysRevLett.100.045504 PACS numbers: 62.50.−p, 61.05.C−, 71.30.+h, 74.62.Fj

Dense monatomic hydrogen is expected to show very unusual physical properties, such as metallic conductivity, high-temperature superconductivity, and quantum liquid state at 0 K [1–4]. Despite enormous experimental efforts, metallic solid hydrogen has never been observed experimentally, even at pressures as high as 320–340 GPa [5–7]. There is another way to create a dense hydrogen-dominant metallic lattice. Ubbelohde suggested that metal-hydrogen alloys might show similar properties to those of metallic hydrogen [8]. Indeed, many transition elements, rare earths, or actinides absorb a significant amount of hydrogen, forming metallic alloys already at ambient pressure, but metallic hydrogen has not been found [9]. In these hydrides, hydrogen atoms are isolated in the interstitial sites of the metal lattice and vibrate predominantly in optical modes which only coupled weakly with conduction electrons. It was suggested recently that a ''hydrogen-dominant'' metallic state might be found under pressure in covalent hydrides, which are insulators at ambient pressure [10]. Contrary to interstitial hydrides, covalent hydrides are very compressible and their volumes are expected to reduce by 50% to 70% at 100 GPa. The strong compression should result in a wide overlap of electronic bands and the hydrides become metallic. Assuming that in the high-pressure metallic phases hydrogen atoms form a three-dimensional net, one would expect to obtain a hydrogen-dominant state having properties similar to metallic hydrogen [10]. No evidence for a metallic state in the covalent ''light'' hydrides has been reported so far. There has been a recent report showing that SiH_4 remains an insulator up to a pressure of 215 GPa [11], whereas theory suggests a superconducting state at pressures above 100 GPa [12]. Here we present the first experimental evidence for a pressure-induced hydrogen-dense metallic state in a light covalent hydride, AlH_3, at 100 GPa.

Six different crystalline forms of AlH_3 have been reported at ambient pressure [13]. Four (α, $\acute{\alpha}$, β, and γ phases) have been synthesized reproducibly and their crystal structures determined [14–18]. These structures are built from AlH_6 octahedrons linked by Al-H-Al bridges. Similar to other hydrides, the first-neighbor metal (M)-H distances (1.7 Å) in the ''bridges'' are much shorter than nearest H-H distances (2.3–2.5 Å). The crystal structure of the most stable modification, α-AlH_3, has been examined by x-ray diffraction up to pressures of 35 GPa [19,20] and by neutrons up to 7.2 GPa [21]. The R-3c structure was found to be stable up to at least 35 GPa. There was the suggestion that this structure and the insulating state will be stable at 100 GPa and above [20]. Prior to the high-pressure study, AlH_3 was examined at ambient pressure by x-ray and neutron diffraction. Only α-AlH_3 was observed without any trace of impurities. High-pressure x-ray diffraction was performed at room temperature in a diamond anvil cell (DAC) at the ID9A high-pressure beam line of the European Synchrotron Radiation Facility in the angular dispersive mode. To ensure quasihydrostatic conditions up to 110 GPa, hydrogen was used as a pressure-transmitting medium. Pressure was measured by the ruby-fluorescent technique. Powder diffraction patterns were analyzed with the FULLPROF software. Resistance and optical measurements were performed at the Max Planck Institute in a DAC using the quasi-four-probe technique with platinum electrodes. No pressure-transmitting medium was used in these measurements. The pressure was determined by ruby fluorescence and from Raman shift of the high-frequency edge of the stressed diamond. The absence of Raman modes associated with molecular hydrogen indicates no hydrogen dissociation up to 164 GPa. The low pressure x-ray results are in agreement with earlier reports [19–21]. A monoclinic distortion of the α phase where Bragg peaks deviated slightly from the calculated positions in the R-3c space group were observed [20]. The deviations possibly originate from a small uniaxial pressure component in the pressure cell, are very small (~0.1%), and did not increase even at 60 GPa. At higher pressure, drastic changes in the diffraction pattern were observed at 63 GPa (Fig. 1). The

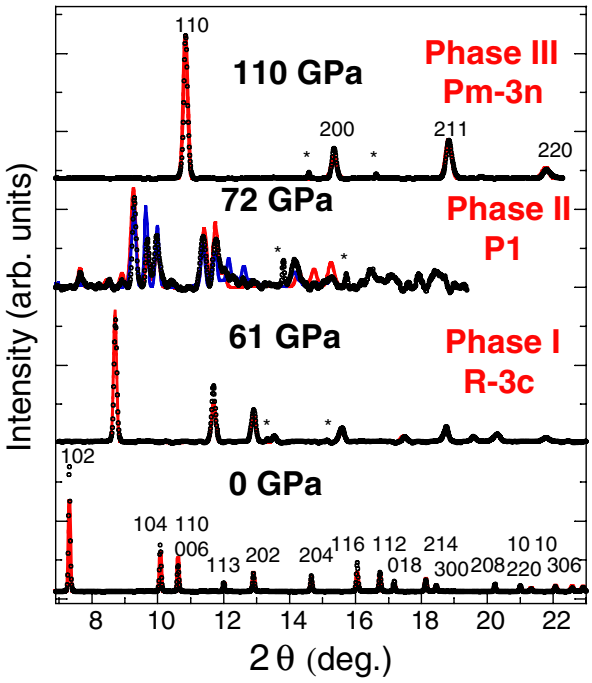

FIG. 1 (color online). X-ray diffraction patterns of phases I, II, and III of AlH_3. Incident wavelength is 0.412 Å. Solid lines are calculated diffraction patterns. Asterisks mark diffraction peaks from the pressure-transmitting medium. The hexagonal ($a = 4.44$ Å, $c = 11.8$ Å) unit cell of phase I at ambient contains 6 formula units, Al in 6b (0, 0, 0) positions and H in 18e (0.63, 0, $\frac{1}{4}$) positions, in agreement with Refs. [14,15]. Phase II at 72 GPa was described in a monoclinic (space group $P2$) unit cell with lattice parameters $a = 3.21$ Å, $b = 6.18$ Å, $c = 2.95$ Å, $\hat{a} = 119.7°$ containing 3 f.u. [solid (red) line] or in a trigonal ($a = 3.83$ Å, $b = 5.12$ Å, $c = 6.72$ Å, $\alpha = 112.6°$, $\beta = 111.9°$, $\gamma = 56.6°$) unit cell (space group $P1$) containing 6 f.u. suggested by theory (blue line). Phase III has a cubic structure with Al atoms in positions (0, 0, 0) and ($\frac{1}{2}, \frac{1}{2}, \frac{1}{2}$), $a = 3.08$ Å at 110 GPa. Bragg R factor for phase III $R_B = 7\%$.

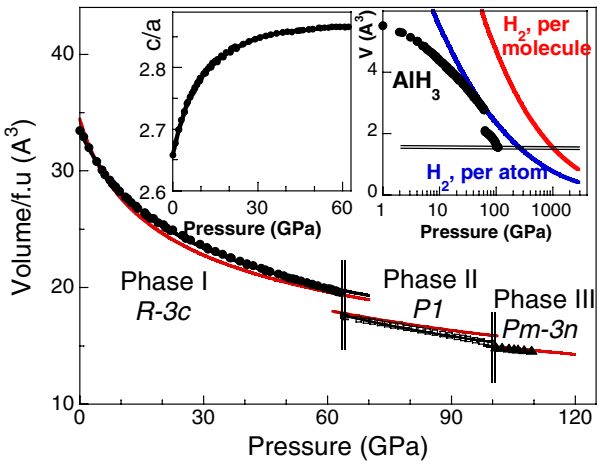

FIG. 2 (color online). Volume per formula unit in AlH_3 as a function of pressure. Black lines are fits of the experimental data by the Murnaghan-Birch equation. The volume of phase II was calculated in the monoclinic model. The fitting parameters are the following: $V_0 = 33.5(1)$ Å, $B_0 = 42.3(5)$ GPa, $B_1 = 3.5(1)$ for phase I; $V_0 = 31.7(5)$ Å, $B_0 = 44.9(10)$ GPa, $B' = 2.7(2)$ for phase II; $V_0 = 27.0(5)$ Å, $B_0 = 50.4(10)$ GPa, $B' = 3.5(2)$ for phase III. Red lines are results from *ab initio* calculations. In insets, left: c/a ratio in phase I versus pressure; right: partial hydrogen volume per H atom in AlH_3 (circles) compared with volume per H atom (blue curve) and per H_2 molecule (red curve) expected in molecular hydrogen. Double line is a guide for the eye.

new phase (phase II) can be described by a monoclinically ($\mathbf{a} \neq \mathbf{b}$ in hexagonal setting) distorted unit cell of the initial R-3c structure (Fig. 1). Nevertheless, displacements of diffraction peaks and discrepancies between measured and calculated intensities suggest that the real symmetry might be lower (i.e., triclinic). A second phase transition (phase III) was observed at 100 GPa (Figs. 1 and 2). At this pressure, the volume of AlH_3 is only 45% of its ambient value. The structure of phase III is remarkably simple and completely different from structures found in other covalent hydrides with two aluminum atoms forming a simple body centered cubic lattice (Fig. 1). The positions of hydrogen atoms cannot be determined from the x-ray data. In a cubic unit cell consisting of 2 f.u., there are two possibilities to locate 6 H atoms. In the first model, H atoms occupy centers of the faces and centers of the edges of the cubic cell. This is the well-known Im-3m ReO_3 type structure. In the second model, H atoms are grouped in pairs and located on faces, forming linear chains along the cubic axes. The symmetry of this structure is Pm-3n. Both structures are characterized by the same H-H distances (1.54 Å at 110 GPa). In the above structures the H-H distances are the same and shorter than the Al-H distances (1.54 and 1.72 Å in the $Im3m$ and Pn-3m structures, respectively). The structural transitions are accompanied by drastic changes in electronic properties. At 60 GPa the sample starts to darken, indicating a gradual transformation to a semiconducting state. At 100 GPa, at the onset of the phase II—phase III structural transformation, the sample becomes black and the electrical resistance shows a remarkably sharp insulator-metal transition (Fig. 3). Variation of electrical resistance in the temperature range 4–300 K shows a typical metallic behavior, but there is no sign of a superconductive transition. Increasing pressure from 100 to 165 GPa does not change the conductivity significantly, and no evidence for another electronic transition was found.

The observation of a hydrogen-dense, highly symmetric, and metallic (while not superconducting) state in the covalent hydride is highly interesting. It has no analogues among known M-H phases. The H-H distances in phase III at 110 GPa are the shortest ever reported except for the H_2 molecule. From the extrapolation of low pressure data, H_2-H_2 distances of the same value are expected in molecular hydrogen at 400 GPa [22]. One can also estimate the

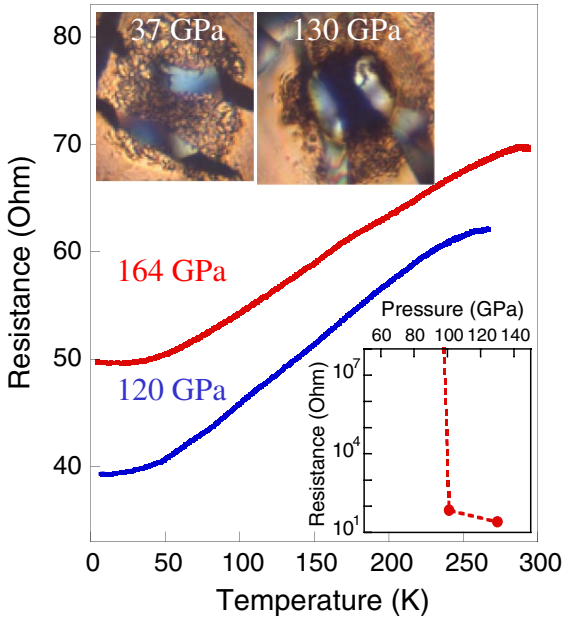

FIG. 3 (color online). Electrical resistance in AlH_3 at the pressures of 120 and 164 GPa as a function of temperature. Residual resistance at the lowest temperature in part originates from the electrical contacts due to the quasi-four-probe technique. In insets, top: image of the sample and the electrical contacts before and after the insulator-metal transition; bottom: electrical resistance measured at room temperature and different pressures.

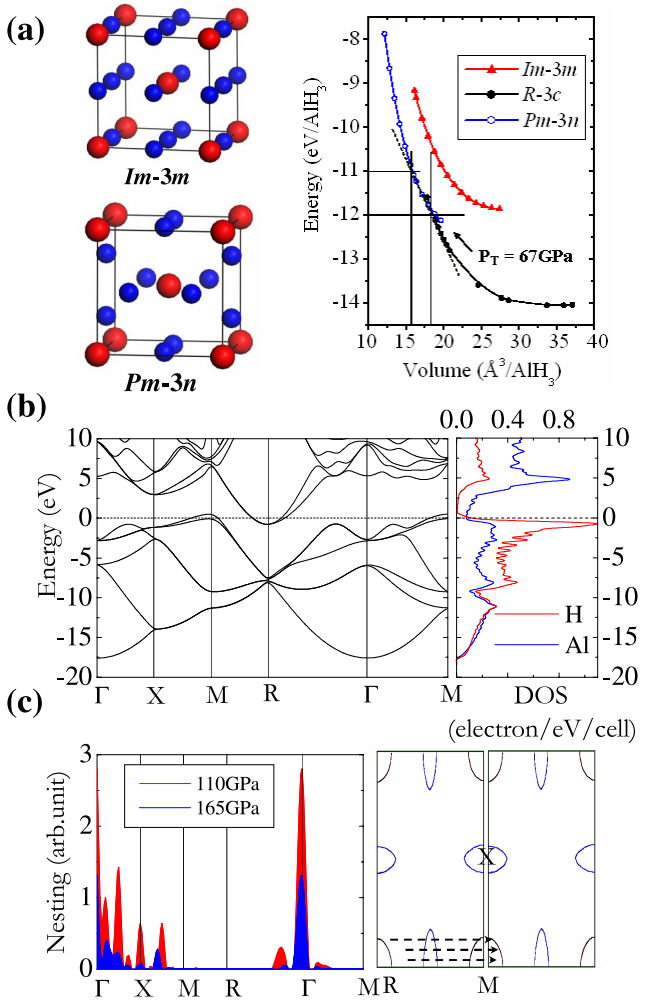

FIG. 4 (color online). (a) Left: the $Im3m$ (up) and Pm-$3n$ (down) structures suggested for phase III. Aluminum atoms are shown in red and hydrogen atoms are shown in blue. Each cell contains 2 f.u., aluminum atoms occupy positions $(0, 0, 0)$ and $(\frac{1}{2}, \frac{1}{2}, \frac{1}{2})$. In the Pm-$3n$ structure, hydrogen atoms occupy positions $(\frac{1}{2}, \frac{1}{4}, 0)$, $(\frac{1}{2}, \frac{3}{4}, 0)$, $(\frac{1}{4}, 0, \frac{1}{2})$, $(\frac{3}{4}, 0, \frac{1}{2})$, $(0, \frac{1}{2}, \frac{1}{4})$, $(0, \frac{1}{2}, \frac{3}{4})$. Right: calculated enthalpy in the R-$3c$, $Im3m$, and Pm-$3n$ structures. (b) Calculated electronic band structure (left) and projected density of states (right) in the Pm-$3n$ phase. (c) Plots of the nesting function at 110 GPa and 165 GPa (left) showing significant nesting in the R–M direction at 110 GPa but diminished at 165 GPa. (Right) Possible nesting vectors connecting the 2 pieces of Fermi surfaces at 110 GPa.

partial "hydrogen" volume in the hydride from subtraction of the atomic volume of pure aluminum [23] measured at the same pressure. This procedure has been widely used for interstitial hydrides. At ambient pressure, the partial hydrogen volume (5.5 $Å^3$) is about twice that in a typical transition metal hydride [24]. At 110 GPa, it drops to only 1.5 $Å^3$. For comparison, a similar volume is expected per H_2 molecule in molecular hydrogen at 800 GPa (see inset of Fig. 2).

The structural stability, electronic structure, and phonon dynamics of AlH_3 under pressure were studied by first principles density functional pseudopotential plane-wave calculations [25]. A structural search using a genetic algorithm found that at pressures above 60 GPa AlH_3 transforms to a lower symmetry and lower enthalpy triclinic structure formed by distorted and shifted triangular Al planes. The predicted lattice parameters [26] and unit cell volumes from 65 to 100 GPa (Figs. 2) fits reasonably well the experimental data (Fig. 1). At pressures above 100 GPa a cubic structure becomes energetically favorable. The Im-$3m$ and Pm-$3n$ hydrogen arrangements described above were examined, and the latter structure was found to be energetically more favorable [Fig. 4(a), right]. The difference in energy is very large (2 eV at 100 GPa) and far exceeds any anticipated error in the calculations. We conclude that the Pm-$3n$ structure is likely to be the structure of phase III. Electronic band structure calculations show that the Pm-$3n$ structure is metallic [Fig. 4(b)]. The calculated valence bandwidth is very broad (17.5 eV) and shows strong hybridization among the Al and H orbitals. Bader topological analysis [27] of the valence charge density have identified bond critical points between H and Al and with neighboring H atoms, although the strength of interaction is weaker in the latter case. Electron-phonon calculations indicate phase III should be superconducting with a mass enhancement parameter $\lambda = 0.74$. Employing

the extended McMillan equation [28] with a nominal Coulomb repulsion parameter $\mu^* = 0.14$ [10], the predicted critical temperature (T_c) is 24 K at 110 GPa. So, why was superconductivity not observed at this temperature experimentally? To answer the question, calculations were extended to higher pressure to study the sensitivity of electron-phonon coupling to the shape of the Fermi surface. At 110 GPa, the strong phonon coupling is dominated by a nesting of the Fermi surface [28,29]. The nesting is extremely sensitive to electron density and pressure [Fig. 4(c)]. At 165 GPa the calculated T_c is only 6 K. It is also found that at 110 GPa, low frequency vibrations ($\sim$220 cm^{-1}), which are close to the estimated superconductivity band gap ($\sim$170–200 cm^{-1}), contribute significantly to the electron-phonon coupling. The role of such a soft phonon mode to superconductivity is still an open issue. They are not present in pure hydrogen, but they might appear in hydrogen-dominant hydrides. It has been suggested [30] that phonon modes with energy close to or less than the superconductivity band gap will decrease the T_c. Removing the low frequency modes from the calculation of the electron-phonon coupling parameter reduces T_c to 6 K at 110 GPa. A larger value of μ^* will reduce the T_c even further. Finally, it appears that the high-T_c superconductivity in hydrogen-dominant alloys is not as straightforward as anticipated [10] and might exist in some ''window'' of parameters such as pressure and electronic density or frequency of low-energy phonon modes [31].

*Corresponding author.
John.Tse@usask.ca

[1] N. W. Ashcroft, Phys. Rev. Lett. **21**, 1748 (1968).
[2] E. G. Browan, Yu. Kagan, and A. Kholas, Sov. Phys. JETP **35**, 783 (1972).
[3] J. E. Jaffe and N. W. Aschroft, Phys. Rev. B **23**, 6176 (1981).
[4] S. A. Bonev, E. Schwegler, T. Ogitsu, and G. A. Galli, Nature (London) **431**, 669 (2004).
[5] H. K. Mao and R. J. Hemley, Rev. Mod. Phys. **66**, 671 (1994).
[6] P. Loubeyre, F. Occelli, and R. LeToulec, Nature (London) **416**, 613 (2002).
[7] Ch. Narayana, H. Luo, J. Orloff, and A. L. Ruoff, Nature (London) **393**, 46 (1998).
[8] A. R. Ubbelohde, Proc. R. Soc. A **159**, 295 (1937).
[9] A. Stritzker and H. Wühl, in *Hydrogen in Metals*, edited by G. Alefeld and J. Völkl, Topics in Applied Physics Vol. 29 (Springer-Verlag, Berlin, 1978), Chap. II, p. 243.
[10] N. W. Ashcroft, Phys. Rev. Lett. **92**, 187002 (2004).
[11] L. Sun, A. L. Ruoff, C. S. Zha, and G. Stupian, J. Phys. Condens. Matter **18**, 8573 (2006).
[12] J. Feng, W. Grochala, T. Jaron, R. Hoffmann, A. Bergara, and N. W. Ashcroft, Phys. Rev. Lett. **96**, 017006 (2006).
[13] F. M. Brower, N. E. Matzek, P. F. Reigler, H. W. Rinn, C. B. Roberts, D. L. Schmidt, J. A. Snover, and K. Terada, J. Am. Chem. Soc. **98**, 2450 (1976).
[14] J. W. Turley and H. W. Rinn, Inorg. Chem. **8**, 18 (1969).
[15] H. W. Brinks, A. Istad-Lem, and B. C. Hauback, J. Alloys Compd. **433**, 180 (2007).
[16] H. W. Brinks, A. I. Lem, and B. C. Hauback, J. Phys. Chem. B **110**, 25833 (2006).
[17] V. A. Yartus, R. V. Denys, J. P. Maehlen, C. Frommen, M. Fichtner, B. M. Bulychev, and H. Emerich, Inorg. Chem. **46**, 1051 (2007).
[18] H. W. Brinks, C. Brown, C. M. Jensen, J. Graetz, J. J. Reilly, and B. C. Hauback, J. Alloys Compd. **441**, 364 (2007).
[19] B. Baranowski, H. D. Hochheimer, K. Strossner, and W. Honle, J. Less-Common Met. **113**, 341 (1985).
[20] J. Graetz, S. Chaudhuri, Y. Lee, and T. Vogt, Phys. Rev. B **74**, 214114 (2006).
[21] I. N. Goncharenko, V. P. Glazkov, A. V. Irodova, and V. A. Somenkov, Physica (Amsterdam) **174B**, 117 (1991).
[22] P. Loubeyre, R. LeToullec, D. Hausermann, M. Hanfland, R. J. Hemley, H. K. Mao, and L. W. Finger, Nature (London) **383**, 702 (1996).
[23] A. Dewaele, P. Loubeyre, and M. Mezouar, Phys. Rev. B **70**, 094112 (2004).
[24] R. Griesse, Phys. Rev. B **38**, 3690 (1988).
[25] Structural determination calculations were performed with electronic structure codes VASP [G. Kresse and J. Furthmüller, Comput. Mater. Sci. **6**, 15 (1996)]. PAW pseudopotentials generated within the generalized-gradient approximation (GGA) exchange correlation functional and distributed with the VASP package were used. Electron-phonon calculations were performed with density functional perturbation theory using the program QUANTUM-EXPRESSO [S. Baroni, S. de Gironcolo, and A. Dal Corso, Rev. Mod. Phys. **73**, 515 (2001)]. The electronic wave function was expanded with a kinetic energy cutoff of 100 Ryd. Monkhorst-Pack meshes [H. J. Monkhorst and J. D. Pack, Phys. Rev. B **13**, 5188 (1976).] were used for Brillouin zone (BZ) integrations in the electronic calculations (k-mesh), and BZ sampling in phonon and electron-phonon coupling (EPC) calculations (q-mesh). EPC matrix elements were computed in the first BZ on a $8 \times 8 \times 8$ q-mesh using individual EPC matrices obtained with a $24 \times 24 \times 24$ k-mesh.
[26] Calculated lattice parameters of the triclinic (space group P1) phase II at 72 GPa: $a = 4.13$ Å, $b = 5.25$ Å, $c = 6.7$ Å, $\alpha = 114.8°$, $\beta = 114.4°$, $\gamma = 53.7°$.
[27] R. F. W. Bader, *Atoms in Molecules—A Quantum Theory* (Oxford University Press, Oxford, 1990).
[28] P. B. Allen and R. C. Dynes, J. Phys. C **8**, L158 (1975).
[29] J. S. Tse, Y. Yao, and K. Tanaka, Phys. Rev. Lett. **98**, 117004 (2007).
[30] A. E. Karakozov, E. G. Maksimov, and S. A. Mashkov, Sov. Phys. JETP **41**, 971 (1976).
[31] J. E. Moussa and M. L. Cohen, Phys. Rev. B **74**, 094520 (2006).